

LETTERS

Superconductivity in alkali-metal-doped picene

Ryoji Mitsuhashi¹, Yuta Suzuki², Yusuke Yamanari², Hiroki Mitamura¹, Takashi Kambe², Naoshi Ikeda², Hideki Okamoto^{3,4}, Akihiko Fujiwara⁵, Minoru Yamaji⁶, Naoko Kawasaki¹, Yutaka Maniwa⁷ & Yoshihiro Kubozono¹

Efforts to identify and develop new superconducting materials continue apace, motivated by both fundamental science and the prospects for application. For example, several new superconducting material systems have been developed in the recent past, including calcium-intercalated graphite compounds¹, boron-doped diamond² and—most prominently—iron arsenides such as LaO_{1-x}F_xFeAs (ref. 3). In the case of organic superconductors, however, no new material system with a high superconducting transition temperature (T_c) has been discovered in the past decade. Here we report that intercalating an alkali metal into picene, a wide-bandgap semiconducting solid hydrocarbon, produces metallic behaviour and superconductivity. Solid potassium-intercalated picene (K_xpicene) shows T_c values of 7 K and 18 K, depending on the metal content. The drop of magnetization in K_xpicene solids at the transition temperature is sharp (<2 K), similar to the behaviour of Ca-intercalated graphite¹. The T_c of 18 K is comparable to that of K-intercalated C₆₀ (ref. 4). This discovery of superconductivity in K_xpicene shows that organic hydrocarbons are promising candidates for improved T_c values.

The metal doping of organic molecular compounds and graphites, solids with π -electron networks, has been extensively studied in the search for novel physical properties, such as metallic behaviour and superconductivity^{1,4-14}. Alkali-metal doping of face-centred cubic (f.c.c.) C₆₀ crystals has produced a T_c as high as 33 K; the maximum T_c was observed in solid RbCs₂C₆₀ (ref. 5). In alkali-metal-doped C₆₀ crystals, expansion of the lattice led to the increase in T_c , which is well explained by the density of states (DOS) on the Fermi level ($N(\epsilon_F)$) being enhanced by the reduction of transfer integral t , which leads to an increased T_c according to the Bardeen, Cooper and Schrieffer (BCS) theorem. A general relationship has been reported between T_c and the lattice constant a of alkali-metal-doped f.c.c. C₆₀ crystals⁶. Nevertheless, no superconductivity has been observed for Cs₃C₆₀ at ambient pressure. In 1995, a superconducting transition of $T_c = 40$ K at the high pressure of 15 kbar was reported⁷ for Cs₃C₆₀ prepared by a solution process with liquid NH₃, but its superconducting volume fraction was quite small. Very recently, a superconducting volume fraction of 80% ($T_c = 38$ K) was reported⁸ for Cs₃C₆₀ at 15 kbar. This was assigned to the A15 phase, and was realized by a solution process involving (CH₃)NH₂ (ref. 8). Its physical properties are fully reported in ref. 9. The metal-doped graphites also show a superconducting transition at ambient pressure. Ca-doped graphite, CaC₆, has¹ a superconducting transition of $T_c = 11.5$ K. Furthermore, Yb-doped graphite, YbC₆, is¹⁰ a superconductor with a T_c of 6.5 K. The metal atoms are intercalated into the space between the graphene sheets. These T_c values are considerably higher than those of alkali-metal-doped graphite reported in the 1960s¹¹. Thus, modification of the electronic structures in materials with π -electron networks by metal doping is a very important way to bring out novel physical properties, such as superconductivity.

Recently, a new synthetic route was found for the organic hydrocarbon, picene¹⁴, the molecular structure of which is shown in Fig. 1. A detailed description of the synthetic method is provided in Supplementary Information. This very simple method can produce large quantities of high purity picene. We have fabricated a field-effect transistor (FET) with thin films of picene synthesized by this procedure¹⁵⁻¹⁷. The FET device showed excellent properties, with a field-effect mobility, μ , of greater than $3 \text{ cm}^2 \text{ V}^{-1} \text{ s}^{-1}$, which is remarkably enhanced by exposure to O₂. These excellent properties are due to its wide bandgap of 3.3 eV (ref. 15). The μ value of the picene thin film FET currently reaches $\sim 5 \text{ cm}^2 \text{ V}^{-1} \text{ s}^{-1}$ under 500 torr of O₂, which is the highest μ reported to date for an organic thin film FET. The picene molecule is a flat hydrocarbon, as can be seen from Fig. 1, and it may be regarded as a fragment of graphene sheet. Therefore, by analogy with the superconductivity of metal-intercalated graphite, we can expect to produce superconductivity by doping picene crystals with a metal. The metal-intercalated compounds of the aromatic hydrocarbon pentacene, with the same number of benzene rings as picene, have been investigated by several groups¹²⁻¹⁴. However, only metallic behaviour was found in alkali-metal-doped pentacene, and no superconducting transition was observed. In this study, we have prepared alkali-metal-intercalated picene solids and investigated their physical properties. The magnetic properties of the K_xpicene solids clearly showed superconducting transitions at 7 and 18 K.

A crude sample of picene was synthesized by the procedure mentioned above¹⁴. The ¹H NMR of this crude sample showed only peaks due to the H atoms of picene. The crude sample was sublimed and purified by heating at 573 K under flowing Ar. The ESR of the sublimed sample showed no peaks, showing that the sublimed picene

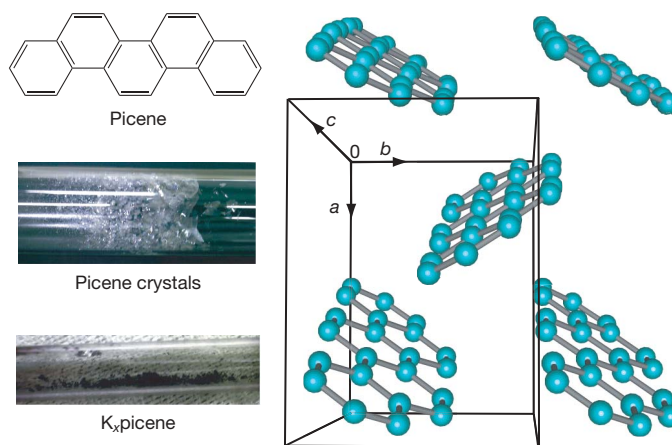


Figure 1 | Molecular structure, crystal structure and physical appearance of picene. Photographs show pristine picene (top; white) and K_xpicene (bottom; black).

¹Research Laboratory for Surface Science, ²Department of Physics, ³Department of Chemistry, Okayama University, Okayama 700-8530, Japan. ⁴Institute for Materials Chemistry and Engineering, Kyushu University, Fukuoka 812-8581, Japan. ⁵Japan Advanced Institute of Science and Technology, Ishikawa, 923-1292, Japan. ⁶Department of Chemistry and Chemical Biology, Gunma University, Kiryu 376-8515, Japan. ⁷Department of Physics, Tokyo Metropolitan University, Hachioji 192-0397, Japan.

sample had no impurities detectable by ESR. Furthermore, the Rietveld refinement for the X-ray diffraction pattern of pristine picene could be achieved based on the crystal structure reported previously¹⁸; the 'herringbone' crystal structure is shown in Fig. 1. The X-ray diffraction pattern of picene is shown in Supplementary Fig. 7a. The alkali metals were intercalated into crystals of picene by annealing nominal compositions of picene and alkali metals in glass tubes at 440 K for 7–21 days. The pressure in the glass tube was reduced to 10^{-6} torr before sealing and annealing. As shown in Fig. 1, the K_x picene sample was a black powder, quite different from the white powder of pristine picene. The chemical stability of K_x picene is fully described in Supplementary Information. In this paper, the x values in alkali-metal-intercalated picene (A_x picene, where A indicates alkali metal) refer to the nominal mole ratios.

Figure 2a shows the magnetization M (expressed as M/H , where H is the applied magnetic field) as a function of temperature T , for $K_{2.9}$ picene for zero field cooling (ZFC) and field cooling (FC) measurements; here H is 20 Oe. Both M/H versus T plots show a drastic decrease below 7.1 K. The explanation how the superconducting transition temperature is determined in this study is fully described in Supplementary Information; the temperature of the inflection point in the M/H versus T plot, T_c^{inf} , is defined as T_c in this text. The T_c was determined to be 7.0 K from these plots. The diamagnetic M/H in the ZFC and FC measurements can be assigned to the shielding and Meissner effects, respectively. As seen from Fig. 2a, the M/H value decreases rapidly, and the difference between T_c^{onset} and the temperature for the minimum M/H value (T_c^{end}) is less than 0.5 K. This is extremely small in comparison with the corresponding value of >10 K for K_3C_{60} and $LaO_{1-x}F_xFeAs$ (refs 3, 4), while a similarly rapid reduction is clearly observed in CaC_6 (ref. 1). The shielding fraction shown in Fig. 2a is $\sim 0.1\%$. The highest shielding fraction reaches 15% in K-doped picene exhibiting a T_c of 7 K, for which the M/H versus T plots are shown in Fig. 2a inset.

In Fig. 2b we show an M/H versus T plot of $K_{3.3}$ picene exhibiting a T_c of 18 K in ZFC and FC measurements at an applied H of 20 Oe. The

M decreases below 20 K, that is, the T_c^{onset} is as high as 20 K; from the inflection point of the plots, the T_c was determined to be 18 K. The diamagnetic M/H is clearly confirmed in the ZFC measurement, and the diamagnetic M/H decreases in the FC measurement. These diamagnetic M/H values can be assigned to the shielding and Meissner effects, demonstrating a superconducting phase in $K_{3.3}$ picene below 18 K. The M/H almost reaches its minimum value within ~ 2 K from the normal state. The shielding fraction is 1.2%. It should be noted that this T_c is extremely high among organic superconductors^{4–8,19}, being even comparable to that of K_3C_{60} (ref. 4). Although the nominal value of x in both $K_{2.9}$ picene and $K_{3.3}$ picene is close to 3, we cannot clearly determine at present whether these differences represent different crystal phases in K_3 picene or different numbers of K atoms intercalated into the picene crystals. Furthermore, it is important to say that both the shielding and Meissner fractions increased when the powder sample was pressed to form a pellet, showing that this superconductivity is not assigned to the surface but to a bulk phase. The physical properties of superconducting K-doped picene are described in Supplementary Information, together with comments on the superconducting phases and the superconducting volume fraction.

Figure 2c shows the magnetic field dependence of M/H versus T plots for the $T_c = 18$ K superconductor, $K_{3.3}$ picene. We see that the diamagnetic signal disappears gradually with the application of H . The drop of M/H was still observed for $K_{3.3}$ picene even at 1,000 Oe, although the T_c^{onset} value decreased to 17 K. This result shows that the superconducting phase is not completely destroyed by the application of a weak H . The M versus H plot for the $T_c = 18$ K superconductor ($K_{3.3}$ picene) at 5 K is shown in Fig. 2d, and the lower critical magnetic field H_{c1} was determined to be 380 Oe, showing that the $K_{3.3}$ picene is a type-II superconductor. The upper critical H , H_{c2} , cannot be definitely determined, but the value seems to be $>10^4$ Oe. The magnetic field dependence of M/H versus T plot for the $T_c = 7$ K superconductor is described in Supplementary Information (Supplementary Fig. 4).

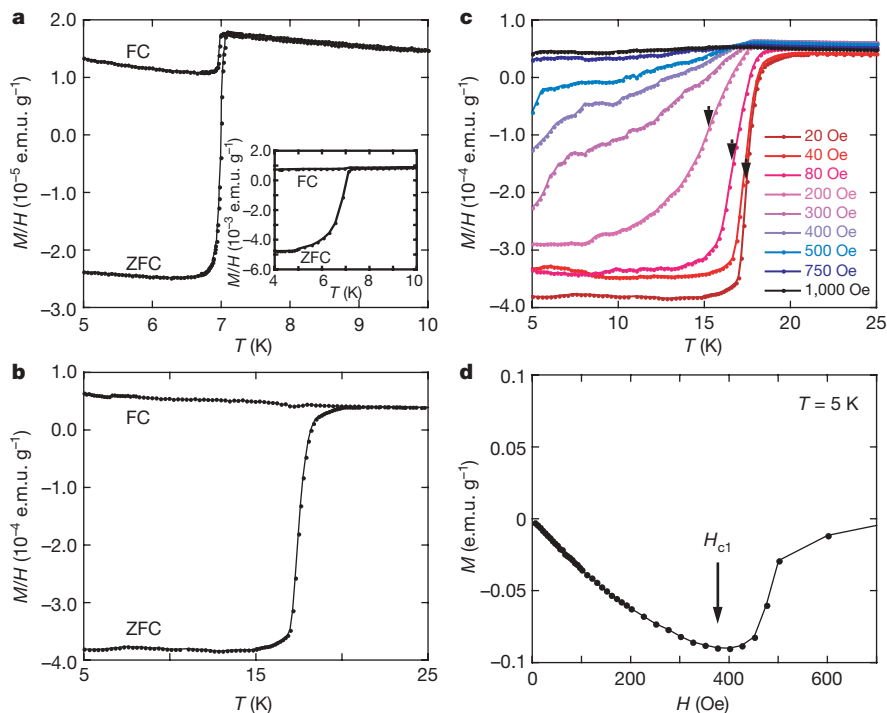


Figure 2 | Temperature dependence of M/H . **a**, M/H versus T plots for superconductors with $T_c = 7$ K; $K_{2.9}$ picene (main) and $K_{3.3}$ picene (inset). The shielding fraction is 0.1% for $K_{2.9}$ picene and 15% for $K_{3.3}$ picene. **b**, M/H versus T plots for the $T_c = 18$ K superconductor, $K_{3.3}$ picene; the shielding fraction is 1.2%. **c**, **d**, Magnetic field dependence of M/H versus T and M

versus H plots for the $T_c = 18$ K superconductor, $K_{3.3}$ picene. The inflection points in M/H versus T plots are shown by black arrows. The M values were measured by SQUID magnetometer (Quantum Design MPMS2) in the temperature region >2 K.

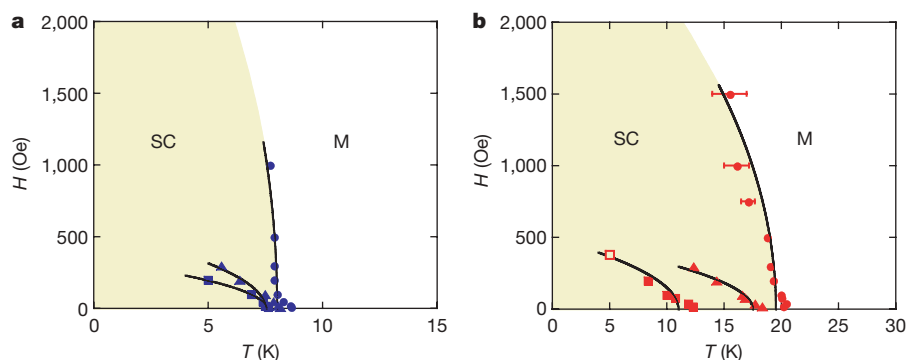


Figure 3 | Superconducting phase diagrams. **a, b,** Superconducting phase diagrams of superconductors with T_c values of 7 K (**a**) and 18 K (**b**). The H versus T plots are determined from the onset temperature (T_c^{onset}) (filled circles), inflection point (filled triangle) and the temperature (filled square)

The superconducting phase diagrams for the superconductors with T_c values of 7 and 18 K are shown in Fig. 3a and b, respectively, and the $(T_c - T)^{1/2}$ fitting curves are also drawn. The plots are estimated from the values of T_c^{onset} , T_c^{inf} ($= T_c$) and T_c^{end} of the M versus T plots for the 7 K superconductor (Supplementary Fig. 4) and the 18 K superconductor (Fig. 2c) at each H . As seen from Fig. 3, the difference between the T_c^{onset} value and the T_c^{inf} (or T_c^{end}) value becomes large with an increase in the applied H , that is, the M versus T plots have a low slope. Here, it should be noted that the H versus T plots (Fig. 3) estimated from T_c^{onset} (filled circles) and T_c^{end} (filled squares) correspond to H_{c2} and H_{c1} , respectively. Actually, as seen from Fig. 3b, the fitting curve for the H versus T plot shown by filled squares is consistent with the H_{c1} value of 380 Oe (shown by the open square) estimated directly from the M versus H plots of $K_{3.3}$ picene at 5 K (Fig. 2d).

The M/H versus T plots above the T_c^{onset} of 7.1 K for the 7 K superconductor and above the T_c^{onset} of 20 K for the 18 K superconductor show a contribution of localized spins in addition to Pauli spins. The magnetic properties of normal states in these superconductors are discussed below with the aid of ESR data. We prepared K_x picene samples with different compositions of K. Some of the prepared K_x picene samples are listed in Table 1 together with their

Table 1 | List of A_x picene (A: alkali-metal) samples prepared in this study

A	x	Annealing temperature (K)	Annealing time (days)	Physical properties	Shielding fraction
K	1.0	440	6.5	Pauli-like	NA
K	1.8	440	7.0	Pauli-like	NA
K	2.6	440	8.0	SC ($T_c = 6.5$ K)	$\ll 0.1\%$
K†	2.9	440	9.0	SC ($T_c = 7.0$ K)	0.1%
K	3.0	440	8.0	SC ($T_c = 6.5$ K)	$\ll 0.1\%$
K	3.0	440	9.0	SC ($T_c = 17$ K)	0.1%
K	3.1	440	4.0	SC ($T_c = 7.4$ K)	$< 0.1\%$
K	3.3	440	21.0	SC ($T_c = 8$ K)	$\ll 0.1\%$
*K‡	3.3	440	21.0	SC ($T_c = 6.9$ K)	15%
K	3.3	440	8.5	SC ($T_c = 7.1$ K)	$\ll 0.1\%$
K	3.3	440	11.0	SC ($T_c = 18$ K)	0.55%
*K§	3.3	440	11.0	SC ($T_c = 18$ K)	1.2%
K	4.0	440	8.0	Curie-like	NA
K	5.1	440	12.5	Curie-like	NA
Na	3.4	570	5.0	Pauli-like	NA
Rb	2.8	440	16.5	Pauli-like	NA
Rb 	3.1	570	6.7	SC ($T_c = 6.9$ K)	10%
Cs	3.0	440	9.0	Metal-insulator transition	NA

Superconducting samples shown bold. The SQUID measurements were generally performed on a powder sample, except as indicated by footnote. SC, superconducting. NA, not available.

* SQUID measurement on pellet samples.

† Properties shown in Figs 2a and 3a, and Supplementary Fig. 3a.

‡ Properties shown in Fig. 2a inset.

§ Properties shown in Figs 2b-d and 3b, and Supplementary Fig. 3b.

|| Properties shown in Supplementary Fig. 3c.

of the minimum value reached in M/H versus T plots at each H ; SC, superconducting phase; M, normal metal phase. The open square refers to the H_{c1} of 380 Oe estimated from M versus H plots (Fig. 2d).

physical properties. All K_x picene samples with $x < 2$ showed Pauli-like behaviour at all temperatures down to 2 K (Supplementary Fig. 5). No superconducting transition was observed for K_x picene with $x < 2$. On the other hand, all K_x picene samples with $x > 4$ showed Curie-like behaviour (Supplementary Fig. 6). These results strongly suggest that the superconducting phase in K_x picene lies on $x \approx 3$, and that different crystal phases exhibiting T_c of 7 and 18 K seem to be formed in K_3 picene. If this is the case, three electrons transferred from K atoms occupy the lowest unoccupied molecular orbital (LUMO) and LUMO+1, and the LUMO+1 is half occupied. Therefore, the DOS of the LUMO+1 band of K_3 picene seems to be responsible for the superconducting transition. The electronic structures of K_x picene are fully described in Supplementary Information.

To extract exclusively the contribution of Pauli paramagnetism, the ESR spectra of K_x picene superconductors were measured. The ESR spectrum consists of a very narrow peak due to localized spins and a wide peak due to conduction electrons (conduction electron ESR). We estimated the magnetic susceptibility to be 7.5×10^{-5} e.m.u. mol^{-1} from the conduction electron ESR for $K_{3.3}$ picene ($T_c = 18$ K) at 300 K, and this gives the $N(\epsilon_F)$ of 1.2 states eV^{-1} per picene per spin. This $N(\epsilon_F)$ value seems to be reliable, because the conduction electron ESR gives selectively only the Pauli paramagnetism. On the other hand, the conduction electron ESR in $K_{2.9}$ picene ($T_c = 7$ K) was too small to estimate the spin susceptibility, suggesting a smaller $N(\epsilon_F)$ for a 7 K superconductor than for a 18 K superconductor. The correlation between $N(\epsilon_F)$ and T_c seems to be reasonable, being consistent with the BCS theorem. The high magnetic susceptibilities in normal states estimated from SQUID (Fig. 2a and b) may be due to additional spins from small amounts of impurities included in the sample. This is fully described in Supplementary Information.

A structure of stacked two-dimensional (2D) layers is formed in pristine picene crystals (herringbone structure), as shown in Fig. 1, and the crystals have a monoclinic lattice (space group $P2_1$) with lattice constants $a = 8.472(2)$ Å, $b = 6.170(2)$ Å, $c = 13.538(7)$ Å and $\beta = 90.81(4)^\circ$; the X-ray diffraction pattern is shown in Supplementary Fig. 7a. The layer forms in the a - b plane, and the 2D layer structure is similar to that of pentacene crystals¹²⁻¹⁴. In the case of alkali-metal-intercalated pentacene, the metal atoms are found to be intercalated in the space between the a - b layers, on the basis of the expansion of c upon intercalation¹²⁻¹⁴. This result is consistent with the very small electric conductivity parallel to the c axis in comparison with conductivity in the a and b directions. We measured the X-ray diffraction pattern of $K_{2.9}$ picene and determined the lattice constants. The Le Bail fitting analysis could reproduce well the measured X-ray diffraction pattern with these lattice constants: $a = 8.707(7)$ Å, $b = 5.912(4)$ Å, $c = 12.97(1)$ Å, $\beta = 92.77(5)^\circ$ —the X-ray diffraction pattern is shown in Supplementary Fig. 7b. The lattice parameters estimated by a simple index analysis showed a good correspondence with the above values determined by means of a Le Bail fit. The a is

expanded from 8.472 to 8.707 Å by the intercalation of K atoms into picene crystals, but the *b* and *c* axes shrunk, suggesting the intercalation of K atoms into the *a*–*b* plane (intralayer intercalation). This is in contrast to the case of lightly doped pentacene^{12–14,20}. The suggested crystal structure of superconducting K_{2.9}picene is fully discussed in Supplementary Information.

Finally, we prepared Na, Rb and Cs intercalated materials, A_{*x*}picene. Pauli paramagnetism was observed down to 2 K for Na_{3.4}picene and Rb_{2.8}picene, while no superconducting transition was observed. The *M/H* of Cs_{3.0}picene changed drastically at around 150 K. Above 150 K, the *M/H* was independent of temperature, while below 150 K the *M/H* increased drastically, indicating a metal–insulator transition at around 150 K. Although the origin of the transition remains to be clarified, the lattice expansion due to the intercalation of Cs atoms, with their large ionic radius, may affect the electronic structure of A_{*x*}picene crystals. Very recently, we observed a clear superconductivity in Rb_{3.1}picene with a *T_c* of 6.9 K and a high shielding fraction of 10% (Supplementary Fig. 3c), and the study of its properties and exact superconducting phase are now in progress. So we have observed superconducting transitions for K_{*x*}picene and Rb_{*x*}picene with *x* ≈ 3. A detailed search for superconductors similar to A_{*x*}picene is necessary to explore further the physics and chemistry of picene and organic hydrocarbon materials.

Received 14 March 2009; accepted 20 January 2010.

- Emery, N. *et al.* Superconductivity of bulk CaC₆. *Phys. Rev. Lett.* **95**, 087003 (2005).
- Ekimov, E. A. *et al.* Superconductivity in diamond. *Nature* **428**, 542–545 (2004).
- Kamihara, Y., Watanabe, T., Hirano, M. & Hosono, H. Iron-based layered superconductor La[O_{1-x}F_x]FeAs (*x* = 0.05 – 0.12) with *T_c* = 26 K. *J. Am. Chem. Soc.* **130**, 3296–3297 (2008).
- Hebard, A. F. *et al.* Superconductivity at 18 K in potassium-doped C₆₀. *Nature* **350**, 600–601 (1991).
- Tanigaki, K. *et al.* Superconductivity at 33 K in Cs_{*x*}Rb_{*y*}C₆₀. *Nature* **352**, 222–223 (1991).
- Fleming, R. M. *et al.* Relation of structure and superconducting transition temperatures in A₃C₆₀. *Nature* **352**, 787–788 (1991).
- Palstra, T. T. M. *et al.* Superconductivity at 40 K in cesium doped C₆₀. *Solid State Commun.* **93**, 327–330 (1995).
- Ganin, A. Y. *et al.* Bulk superconductivity at 38 K in a molecular system. *Nature Mater.* **7**, 367–371 (2008).
- Takabayashi, Y. *et al.* The disorder-free non-BCS superconductor Cs₃C₆₀ emerges from an antiferromagnetic insulator parent state. *Science* **323**, 1585–1590 (2009).
- Weller, T. E. *et al.* Superconductivity in the intercalated graphite compounds, C₆Yb and C₆Ca. *Nature Phys.* **1**, 39–41 (2005).
- Hannay, N. B. *et al.* Superconductivity in graphitic compounds. *Phys. Rev. Lett.* **14**, 225–226 (1965).
- Minakata, T. *et al.* Conducting thin films of pentacene doped with alkaline metals. *J. Appl. Phys.* **74**, 1079–1082 (1993).
- Matsuo, Y., Sasaki, S. & Ikehata, S. Stage structure and electrical properties of rubidium-doped pentacene. *Phys. Lett. A* **321**, 62–66 (2004).
- Kaneko, Y., Suzuki, T., Matsuo, Y. & Ikehata, S. Metallic electrical conduction in alkaline metal-doped pentacene. *Synth. Met.* **154**, 177–180 (2005).
- Okamoto, H. *et al.* Air-assisted high-performance field-effect transistor with thin films of picene. *J. Am. Chem. Soc.* **130**, 10470–10471 (2008).
- Kawasaki, N. *et al.* Trap states and transport characteristics in picene thin film field-effect transistor. *Appl. Phys. Lett.* **94**, 043310 (2009).
- Kaji, Y. *et al.* High-performance C₆₀ and picene thin film field-effect transistors with conducting polymer electrodes in bottom contact structure. *Org. Electron.* **10**, 432–436 (2009).
- De, A., Ghosh, R., Roychowdhury, S. & Roychowdhury, P. Structural analysis of picene, C₂₂H₁₄. *Acta Crystallogr. C* **41**, 907–909 (1985).
- Schirber, J. E. *et al.* Pressure-temperature phase diagram, inverse isotope effect, and superconductivity in excess of 13 K in κ-(BEDT-TTF)₂Cu[N(CN)₂]Cl, where BEDT-TTF is bis(ethylenedithio)tetrathiafulvalene. *Phys. Rev. B* **44**, 4666–4669 (1991).
- Hansson, A., Bohlin, J. & Stafstrom, S. Structural and electronic transitions in potassium-doped pentacene. *Phys. Rev. B* **73**, 184114 (2006).

Supplementary Information is linked to the online version of the paper at www.nature.com/nature.

Acknowledgements The X-ray diffraction patterns were measured with synchrotron radiation at KEK-PF (proposal no. 2007G612), Tsukuba, Japan. This work was supported in part by Grants-in-Aid 20045012 and 18340104 from MEXT, Japan.

Author Contributions R.M., Y.S., Y.Y. and H.M. contributed equally to the preparation of superconducting picene materials and to the performance of magnetic susceptibility measurements with the assistance of T.K. and Y.K.; H.O. and M.Y. synthesized high-quality picene; N.K. and Y.M. provided assistance with X-ray diffraction measurements; N.I. and A.F. provided discussions and suggestions for the overall project, and discussed the experimental data with T.K. and Y.K.; Y.K. was responsible for the overall project direction, planning and integration among different research units.

Author Information Reprints and permissions information is available at www.nature.com/reprints. The authors declare no competing financial interests. Correspondence and requests for materials should be addressed to Y.K. (kubozono@cc.okayama-u.ac.jp).